# The response of mechanical and electronic properties of graphane to the elastic strain

M. Topsakal,[1,a)] S. Cahangirov,[1] and S. Ciraci[1,2]
[1]UNAM-Institute of Materials Science and Nanotechnology, Bilkent University, Ankara 06800, Turkey
[2]Department of Physics, Bilkent University, Ankara 06800, Turkey

Based on first-principles calculations, we resent a method to reveal the elastic properties of recently synthesized monolayer hydrocarbon, graphane. The in-plane stiffness and Poisson's ratio values are found to be smaller than those of graphene, and its yielding strain decreases in the presence of various vacancy defects and also at high ambient temperature. We also found that the band gap can be strongly modified by applied strain in the elastic range. © 2010 American Institute of Physics. [doi:10.1063/1.3353968]

Two-dimensional (2D) monolayer honeycomb structures of graphene,[1,2] BN,[3] and silicon[4] offer remarkable properties and are promising materials for future applications. Honeycomb structure of graphene with $sp^2$ bonding underlies the unusual mechanical properties providing very high in-plane strength. Graphene and its rolled up forms, carbon nanotubes are among the strongest and stiffest materials yet discovered in terms of tensile strength and elastic modulus.[5,6] Graphane, another member of honeycomb structures was theoretically predicted[7] and recently synthesized by exposing graphene to hydrogen plasma discharge.[8] Here each carbon atom being bonded to one hydrogen atom is pulled out from the graphene plane and hence whole structure is buckled. Instead of being a semimetal like graphene, graphane is a wide band gap semiconductor and can attain permanent magnetic moment through hydrogen vacancies.[9]

In this work, we revealed the relevant elastic constants of graphane using strain energy calculations in the harmonic elastic deformation range and compared them with those calculated for other honeycomb structures. We also found that in the presence of hydrogen vacancy and carbon+hydrogen divacancy, its yielding occurs at smaller strains. Furthermore, its band gap first increases then decreases steadily with the increasing applied strain. We believe that our predictions are relevant for the current research focused on the electronic properties of honeycomb structures under strain.[10,11]

First-principles plane wave calculations are carried out within density functional theory using projector-augmented wave potentials.[12] The exchange correlation potential is approximated by generalized gradient approximation (GGA) using PW91 functional. A plane-wave basis set with kinetic energy cutoff of 450 eV is used. All atomic positions and lattice constants are optimized by using the conjugate gradient method, where the total energy and atomic forces are minimized. Interactions between adjacent graphane layers in supercell geometry is hindered by a large spacing of $\sim 10$ Å. To correct the energy bands and band gap values obtained by GGA, frequency-dependent $G_0W_0$ calculations are carried out. $G_0W_0$ corrections are obtained by using $(12 \times 12 \times 1)$ **k**-points in the Brillouin zone (BZ), 400 eV cut-off potential for $G_0W_0$, 160 bands, and 64 frequency grid points. All nu-

merical calculations are performed by using VASP package.[13,14]

The graphene has a 2D hexagonal unit cell with a lattice constant of $a = 2.47$ Å. The C–C bond length is $d = 1.42$ Å and all atoms lie in the same plane. Upon hydrogenation, the lattice constant increases to 2.54 Å and $d$ increases to 1.53 Å. Moreover, C–H bonds are 1.11 Å and the amount of buckling between the alternating carbon atoms in a hexagon is 0.46 Å. Atomic configuration of graphene and graphane structures are shown in Fig. 1(a).

The elastic properties of homogeneous and isotropic materials can be represented by two independent constants,
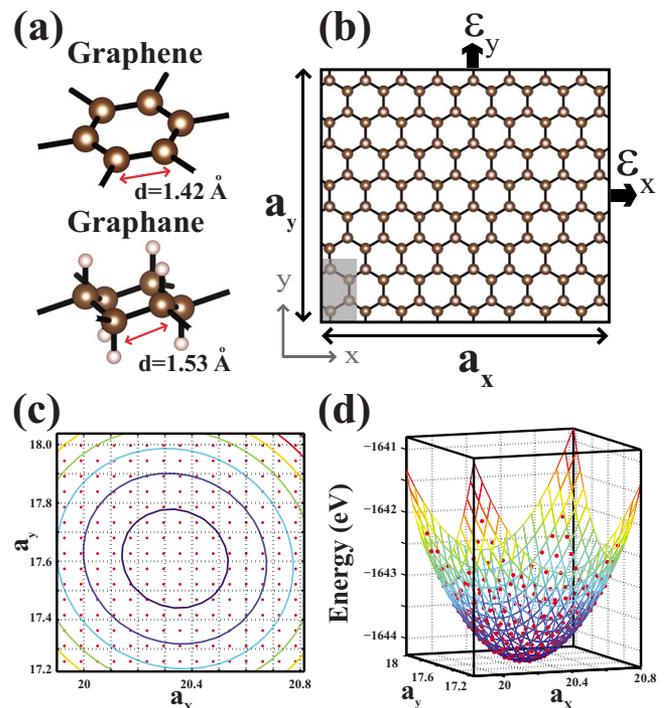


FIG. 1. (Color online) (a) Schematic representation of the atomic structure of graphene and graphane. (b) $(8 \times 4)$ rectangular supercell configuration of the system containing 128 C-H pairs used for the calculation of the elastic constants. $a_x$ and $a_y$ are the lattice constants of the supercell in $x$- and $y$-directions. Shaded region is the smallest unit cell. (c) The mesh of data points $(a_x, a_y)$ used for the total energy calculations. The units are given in angstroms. (d) The three-dimensional plot of $a_x, a_y$ and corresponding total energy values. The red balls are actual points and the lines are the fitted formula.

a)Electronic mail: topsakal@nano.org.tr.

Young's modulus $Y$ and Poisson's ratio $\nu$. Since the thickness of a monolayer structure $h$ is ambiguous, the in-plane stiffness $C$ is a better measure of the strength rather than Young's modulus. Defining $A_0$ as the equilibrium area of the system, the in-plane stiffness can be given as, $C=(1/A_0) \times ((\partial^2 E_S / \partial \epsilon^2))$, where $E_S$ is the strain energy calculated by subtracting the total energy of the strained system from the equilibrium total energy and $\epsilon$ is the uniaxial strain ($\epsilon=\Delta a/a$, $a$ being the lattice constant). The Poisson's ratio which is the ratio of the transverse strain to the axial strain can be defined straightforwardly as $\nu=-\epsilon_{trans}/\epsilon_{axial}$.

For calculation of elastic constants of graphane, we consider large supercell comprising 32 rectangular unit cells ($8\times4$). The calculations are also repeated in ($2\times1$), ($4\times2$), and ($6\times3$) supercells and the obtained results are almost identical, since no reconstructions are observed in the system. Figure 1(b) shows the supercell used in the calculations. $a_x$ and $a_y$ are the lattice constants of the supercell in $x$- and $y$-directions in any strain condition. In the harmonic region, $a's$ are varied with the strain values between $+/-0.02$. A grid data ($a_x;a_y$) containing 225 points is obtained as shown in Fig. 1(c). For each grid point, the corresponding supercell is fully optimized and its total energy is calculated as shown in Fig. 1(d). By using the least-squares method, the data is fitted to the formula, $E_S=a_1\epsilon_x^2+a_2\epsilon_y^2+a_3\epsilon_x\epsilon_y$; where $\epsilon_x$ and $\epsilon_y$ are the small strains along $x$- and $y$-directions in the harmonic region. As a result of isotropy in the honeycomb symmetry, $a_1$ is equal to $a_2$. The same equation can be obtained from elasticity matrix[15] in terms of elastic stiffness constants, namely, $a_1=a_2=(h\cdot A_0/2)\cdot C_{11}$; $a_3=(h\cdot A_0)\cdot C_{12}$. Hence one obtains Poisson's ratio $\nu$ which is equal to $C_{12}/C_{11}=a_3/2a_1$. Similarly, the in-plane stiffness, $C=h\cdot C_{11}\cdot[1-(C_{11}/C_{12})^2]=[2a_1-(a_3)^2/2a_1]/(A_0)$. The calculated values of $C$ by using the present method for graphane, graphene, BN, Si, and SiC 2D honeycomb structures are, respectively, 243, 335, 267, 62, and 166 J/m$^2$. Also the calculated Poisson's ratios are 0.07, 0.16, 0.21, 0.30, and 0.29. Our calculated value of the in-plane stiffness of graphene is in good agreement with the experimental value[5] of $340\pm50$ N/m and justifies the reliability of our method. As seen from the calculated values, the change of the bonding type from $sp^2$ to $sp^3$ and buckling of the atoms in graphane structure makes it 27% less stiffer than graphene. This difference can be used to distinguish graphene and graphane materials. Also the Poisson's ratio of graphane is almost half of the Poisson's ratio of graphene, since the buckled structure of graphane reduces the transverse contraction. Note that depending on their types and concentrations the defects can alter the above elastic constants. For example, a $C_2H_2$-vacancy for the structure in Fig. 1(b) breaks the isotropy and can reduce $C$ by $\sim12\%$ in a specific direction. Hydrogen frustration[8,16] can also be a crucial type of defect, which would affect $C$, since the structure is locally compressed and $A_0$ is influenced.

We next consider the behavior of the system for higher values of the strain ranging from $-0.02$ to 0.45 in uniform expansion. For this purpose, we preferred a fully symmetric hexagonal lattice with well defined high symmetry points in the BZ. Again the calculations are performed in a large ($10\times10$) supercell as shown in Fig. 2(a). The harmonic region can be taken between $-0.02<\epsilon<0.02$ and it is followed by an anharmonic region where higher order terms are
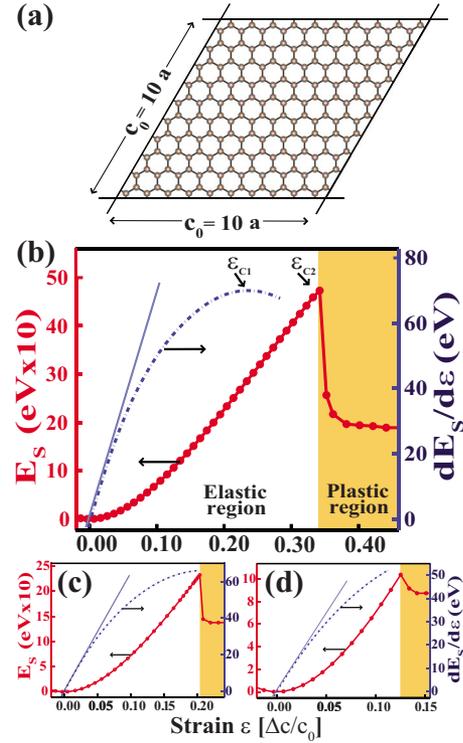


FIG. 2. (Color online) 2D graphane under uniform expansion. (a) Initial atomic configuration in a ($10\times10$) supercell treated with periodic boundary condition. (b) The variation in strain energy $E_S$ and its derivative. The orange/shaded region indicating the plastic range. Strains corresponding to two critical points in the elastic range are labeled as $\epsilon_{c_1}$ and $\epsilon_{c_2}$. (c) Similar to (b) for a single H-vacancy in a ($10\times10$) supercell. (d) For C+H-divacancy in a ($10\times10$) supercell.

not negligible in the strain energy equation. The anharmonic region is followed by a plastic region where irreversible structural changes occur in the system and it transforms into a different structure after the yielding point. Figure 2(b) is the plot of strain energy $E_S$ and its derivative $[dE_S(\epsilon)/d\epsilon]$ with respect to the applied strain. Two critical strain values can be deduced from the plots. The first one, $\epsilon_{c_1}$, is the point where the derivative curve attains its maximum value and then starts to decrease. It occurs nearly at $\epsilon=0.23$, where the C–C bond length is around 1.87 Å. This means that for $\epsilon > \epsilon_{c_1}$, the structure can be expanded under smaller tensions. The phonon frequencies, we calculated by using the force constant method[17] are all positive throughout the BZ for $\epsilon < \epsilon_{c_1}$, but the frequencies of longitudinal acoustic modes start to become imaginary for $\epsilon > \epsilon_{c_1}$, indicating an instability of 2D graphane under uniform expansion beyond $\epsilon_{c_1}$. Such phenomena is known as "phonon instability,"[18,19] where phonon frequencies $\Omega_n(\mathbf{k})$, get imaginary for specific wave vector $\mathbf{k}$ and branch index $n$. A detailed discussion can be found in Ref. 18 and the references therein. Liu et al.[18] calculated the critical strain values for graphene as 0.194 and 0.266 for uniaxial tension in zigzag ($x$-) and armchair ($y$-) directions by using density functional perturbation theory.

The second critical point $\epsilon_{c_2}$ is the yielding point which is around $\epsilon=0.34$. The C–C distance corresponding to $\epsilon_{c_2}$ is 2.02 Å. Up to this point, the strain energy always increases and the system preserves its honeycomblike structure. Upon the release of the tension, all the deformation disappears and hence the system may return to its original size at $\epsilon=0$. Fur-
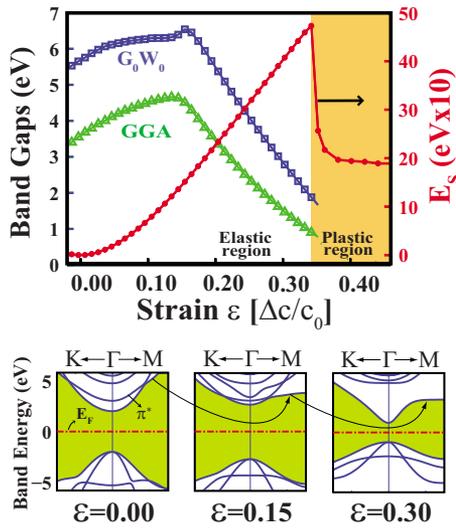
FIG. 3. (Color online) The variation in energy band gaps with (2D) uniform expansion. The band gaps obtained both from GGA (green triangles) and $G_0W_0$ (blue squares) calculations increase with increasing strain up to $\epsilon=0.15$, passes through a maximum, then decrease until the yielding point. The band gaps are given on the left and the strain energies are given on the right. Three panels show how the bands at the edge of conduction band are modified with strain.

thermore, the value of $\epsilon_{c_2}$ is found to depend on various defects and the temperature of the system. For H-vacancy, we found that $\epsilon_{c_2}$ is lowered to $\sim 0.21$ as shown in Fig. 2(c). As for C+H-vacancy, which corresponds to a hole at one corner of hexagon, $\epsilon_{c_2}$ is further lowered to 0.13 as shown in Fig. 2(d). We also examined the effect of ambient temperature on the yielding strain. *Ab initio* molecular dynamic calculations (lasting 2 ps with time steps of $2 \times 10^{-15}$ s) indicate that $\epsilon_{c_2}=0.34$ corresponding to T=0 K is reduced to 0.20 at T=300 K and is further reduced to 0.18 at T =600 K. Apparently, the yielding of perfect graphane under uniform strain at $\epsilon_{c_2}$ can only occur for ideal conditions. For $\epsilon_{c_1} < \epsilon < \epsilon_{c_2}$ the system is in a metastable state. The long wavelength perturbations, vacancy defects, as well as high temperature effects lead $\epsilon_{c_2}$ decrease to the strain values around $\epsilon_{c_1}$. After the yielding point, where $\epsilon \geq \epsilon_{c_2}$, the plastic range sets in with irreversible deformations. This range, however, is beyond the scope of this paper.

We finally investigate the variation in the electronic properties of graphane with the uniform strain. The effect of strain on the buckling is found to be minute. It decreases from 0.46 to 0.43 Å as $\epsilon$ increases from 0 to 0.30. Also, C–H bonds are shortened only 1% in this range of strain. The binding energy of a single hydrogen in $(10 \times 10)$ supercell increases from 4.79 to 5.02 up to $\epsilon=0.20$. Normally, graphane is a semiconductor with a wide direct band gap of 3.54 eV calculated by DFT-GGA, but our calculations show that this gap can increase to 5.66 eV after $G_0W_0$ corrections.

On the other hand, recent $GW_0$ (5.97 eV) (Ref. 9) and $GW$ (5.4 eV) (Ref. 20) corrections report slightly different values depending on the method and parameters used. More recently DFT-LDA calculations[21] found the band gap as 3.6 eV. Figure 3 shows the variation in GGA and $G_0W_0$ band gap values with respect to the strain for uniform expansion in the elastic region. While the lowest conduction band is raised with strain in the first and second panels; in the third panel, the second $\pi^*$ band is lowered steadily and dips in the gap for $\epsilon > 0.15$. Dramatic variation in the band gap with the strain suggests that graphane can be used as a strain gauge at nanoscale.

In summary, we revealed the elastic constants of graphane indicating that it has a quite high in-plane stiffness and very low, perhaps the lowest Poisson's ratio among known monolayer honeycomb structures. We showed that the band gap of graphane can be modified significantly by applied strain in the elastic range. It is suggested that elastic deformation can be used for further functionalization of graphane and hence for monitoring its chemical and electronic properties.

[1] K. S. Novoselov, A. K. Geim, S. V. Morozov, D. Jiang, Y. Zhang, S. V. Dubonos, I. V. Grigorieva, and A. A. Firsov, Science **306**, 666 (2004).
[2] Y. Zhang, Y.-W. Tan, H. L. Stormer, and P. Kim, Nature (London) **438**, 201 (2005).
[3] C. Jin, F. Lin, K. Suenaga, and S. Iijima, Phys. Rev. Lett. **102**, 195505 (2009).
[4] S. Cahangirov, M. Topsakal, E. Akturk, H. Şahin, and S. Ciraci, Phys. Rev. Lett. **102**, 236804 (2009).
[5] C. Lee, X. Wei, J. W. Kysar, and J. Hone, Science **321**, 385 (2008).
[6] Q. Zhao, M. B. Nardelli, and J. Bernholc, Phys. Rev. B **65**, 144105 (2002).
[7] J. O. Sofo, A. S. Chaudhari, and G. D. Barber, Phys. Rev. B **75**, 153401 (2007).
[8] D. C. Elias, R. R. Nair, T. M. G. Mohiuddin, S. V. Morozov, P. Blake, M. P. Halsall, A. C. Ferrari, D. W. Boukhvalov, M. I. Katsnelson, A. K. Geim, and K. S. Novoselov, Science **323**, 610 (2009).
[9] H. Şahin, C. Ataca, and S. Ciraci, Appl. Phys. Lett. **95**, 222510 (2009).
[10] V. M. Pereira and A. H. Castro Neto, Phys. Rev. Lett. **103**, 046801 (2009).
[11] M. Topsakal and S. Ciraci, Phys. Rev. B **81**, 024107 (2010).
[12] P. E. Blöchl, Phys. Rev. B **50**, 17953 (1994).
[13] G. Kresse and J. Furthmuller, Phys. Rev. B **54**, 11169 (1996).
[14] M. Shishkin and G. Kresse, Phys. Rev. B **74**, 035101 (2006).
[15] J. F. Nye, *Physical Properties of Crystals* (Clarendon, Oxford, 1985).
[16] M. Z. S. Flores, P. A. S. Autreto, S. B. Legoas, and D. S. Galvao, Nanotechnology **20**, 465704 (2009).
[17] D. Alfè, Comput. Phys. Commun. **180**, 2622 (2009).
[18] F. Liu, P. Ming, and J. Li, Phys. Rev. B **76**, 064120 (2007).
[19] X. Wei, B. Fragneaud, C. A. Marianetti, and J. W. Kysar, Phys. Rev. B **80**, 205407 (2009).
[20] S. Lebègue, M. Klintenberg, O. Eriksson, and M. I. Katsnelson, Phys. Rev. B **79**, 245117 (2009).
[21] L. Liu and Z. Shen, Appl. Phys. Lett. **95**, 252104 (2009).